

Hexagonal Disk Structures Obtained during Carbonization of *Botryococcus braunii* Residues

Aohan Wang¹, Mikihide Demura², Makoto M. Watanabe², Hiromasa Goto^{1*}

¹Division of Materials Science, Faculty of Pure and Applied Sciences, University of Tsukuba, Tsukuba, Japan

²Algae Biomass and Energy System R & D Center (ABES), University of Tsukuba, Tsukuba, Japan

Email: gotoh@ims.tsukuba.ac.jp

How to cite this paper: Wang, A., Demura, M., Watanabe, M.M. and Goto, H. (2017) Hexagonal Disk Structures Obtained during Carbonization of *Botryococcus braunii* Residues. *Journal of Materials Science and Chemical Engineering*, 5, 22-34. <https://doi.org/10.4236/msce.2017.52003>

Received: December 28, 2016

Accepted: February 10, 2017

Published: February 13, 2017

Copyright © 2017 by authors and Scientific Research Publishing Inc.

This work is licensed under the Creative Commons Attribution International License (CC BY 4.0).

<http://creativecommons.org/licenses/by/4.0/>



Open Access

Abstract

In this study, we report a two-dimensional (2D) hexagonal disk obtained by carbonization of *Botryococcus braunii* (*B. braunii*) residues. Carbonization at 700°C followed by naturally cooling down to room temperature under a non-inert gas flow atmosphere affords to yield this unique structure. The 2D hexagonal disks consist of more than 52% carbon and more than 25% oxygen. Slight amount of Fe, silicon and magnesium would be the trigger of the formation of hexagonal structure. Treatment of biomass residue is a challenge in the near future accompanied by the achievement of new energy technology in the industrial level. This research points out that efficient use of discharged biomass residue could create a new avenue for material science. The morphology of obtained crystals carbonized in different conditions, especially with the existence of argon flow, was also investigated.

Keywords

Hexagonal Disk, Microalgae Residue, *Botryococcus braunii*, Carbonization Condition, Crystal

1. Introduction

Microalgae is well studied in recent years for the promising possibility to be used as new energy stock [1]-[10]. *B. braunii* is especially expected due to the exceedingly high oil productivity. Shimamura *et al.* have successfully achieved a fundamental outdoor culture system of *B. braunii* and an outdoor mass cultivation system of *B. braunii* has been operated in Algae Biomass and Energy System R & D Center (ABES), University of Tsukuba [11]. Mass culture of microalgae inescapably generates a large amount of biomass residues after process. In these five years, studies considering the efficient use of biomass residues have been gradually reported, such like microalgae residue based carbon solid acid catalyst for

biodiesel production [12], methane production from lipid-extracted biomass residues [13] and kinetic study of microalgae residues in pyrolysis [14] [15]. Since biomass residues might be the environmental problems in the near future, research on biomass residues is necessary with increasing demand of the new energy. From the point of view of material science, biomass residues containing much amount of different components are interesting materials. In this study, we adopted *B. braunii* residues as a starting material. Carbonization of the bulk sample in a certain condition affords to yield hexagonal crystals. 2D hexagonal crystals with high anisotropy and large surface area are promised to be the building blocks for functional materials.

In our previous study, we reported that different carbonization condition would affect the morphology of the yielded crystals [16]. Polygonal grains were observed in the sample carbonized above 700°C under argon atmosphere. In this study, we carbonized the *B. braunii* residue at 700°C with no argon flow. Thus obtained samples have hexagonal disks on the surface. We observed these structures by scanning electron microscopy. The side length of these hexagonal disks ranges from several hundred nanometers to one micrometers. This is the first paper reporting the hexagonal disk shaped crystals generated during the carbonization of *B. braunii* residue and any other biomass residues. The crystals were found only in a very limited area of the bulk sample. We performed the infrared absorption spectroscopy, X-ray photoelectron spectroscopy and energy dispersive X-ray spectrometry to analyze the chemical components included inside the sample. Mechanism of the formation of hexagonal disks and role of argon flow are discussed.

2. Experimental

2.1. Preparation of *B. braunii* Residues Samples

The original sample *B. braunii* strain (BOT-22) was isolated from the Okinawa prefecture, Japan and is cultivated in University of Tsukuba [17]. This strain is classified race B and produces botryococcene (C₃₄H₅₈) as a main component of hydrocarbons [18]. The *B. braunii* residue samples were prepared as follows. A mass culture system of *B. braunii* developed in University of Tsukuba provided culture broth of the BOT-22 strain of *B. braunii* for this work [11]. The broth of the BOT-22 was concentrated by using PSI as flocculants and dried by sunlight [19]. The dried sample of the *B. braunii* was soaked into n-hexane for extraction of hydrocarbon oils including a small amount of carotenoids and triacylglycerols. After the extraction, the residual sample was recovered by filtration and then dried again. The obtained materials are plate-like shape with some thickness, and show greenish dark brown color in bulk state.

2.2. Carbonization

B. braunii residues were set in a quartz dish and placed into an Electric Gold Furnace instrument produced by Massachusetts Institute of Technology (MIT) Lincoln-Lab. equipping with an Ishikawa temperature controller and a handmade

furnace assembled by Dr. Shinichi Ito (University of Tsukuba). 200 V of voltage was applied and uniformly heated the interior of furnace. Carbonization was performed with no argon flow from room temperature to 700°C. Then the sample was naturally cooled to room temperature. The carbonized sample was obtained in bulk state with no fragments.

3. Results and Discussion

3.1. SEM Observation

We have mentioned in our previous report that the syngas such like hydrogen gas or carbon monoxide gas would be the trigger of the reduction reaction for the formation of polygonal crystal which consists of Fe_3O_4 or $\alpha\text{-Fe}$ inside [16]. **Figure 1(a)** shows the very beginning stage of the formation of polygonal crystal, observed in the bulk *B. braunii* residues carbonized at 700°C under argon atmosphere. The octahedral shaped crystals imbedded in the sample are clear evidence that reduction reaction occurred. However, the absence of inert gas flow caused a totally different result during the carbonization. In **Figure 1(b)**, hexagonal disk shaped crystals in different sizes were found on the surface and inside of carbonized *B. braunii* residues. These samples were also carbonized at 700°C, only the argon flow was stopped initially. A simple diagram summarized as **Figure 1(c)** shows the difference of the carbonization condition would cause the different crystal shape.

The hexagonal disks were carefully observed under SEM, as shown in **Figure 2**. The length of one side of the hexagon ranges from several nanometers to one micrometer. **Figure 2(a)** is a hexagonal disk with bottom part broken. It is interesting to find the crack of this defect is composed of two straight lines; both are almost parallel to the sides of the original hexagonal disk. In **Figure 2(b)**, the hexagonal disk imbedded perpendicular to the surface of the bulk sample, only half of the hexagon could be observed. We assume this figure indicates that the hexagonal crystal is still under growing process. Most of the hexagonal disks were found like in **Figure 2(c)** and **Figure 2(d)**, which hexagonal disks solitarily attach on the carbonized sample. **Figure SI1** shows a SEM image of the bulk sample with some hexagonal disks adhering on the surface. Some of the hexagonal disks have thickness more than 100 nm (See **Figure SI2(a)**, **Figure SI2(b)**). Magnification shows a part of the hexagonal disk was separated (**Figure SI2(c)**). Two hexagonal disks attached to each other were also observed under SEM, as shown in **Figure SI2(d)** **Figure SI2(e)**. In **Figure SI2(d)**, two hexagonal disks with a very small hexagon were found on the edge of bulk sample, indicating that the crystals are on the process of growth. A similar pattern was also found in **Figure SI2(e)** that two hexagons with one side length of 500 nm attach to each other. **Figure SI2(f)** shows a zigzag edge resembling the external form of honeycomb structure and that of double hexagon disks observed in **Figure SI2(e)**. In **Figure SI2(g)**, a hexagonal disk with a defect that three sides are parallel to the side of original hexagonal disk was observed. A crystal with a round hole was found (See **Figure SI2(h)**). In **Figure SI2(i)**, a hexagon shape-like hole was found on the surface of

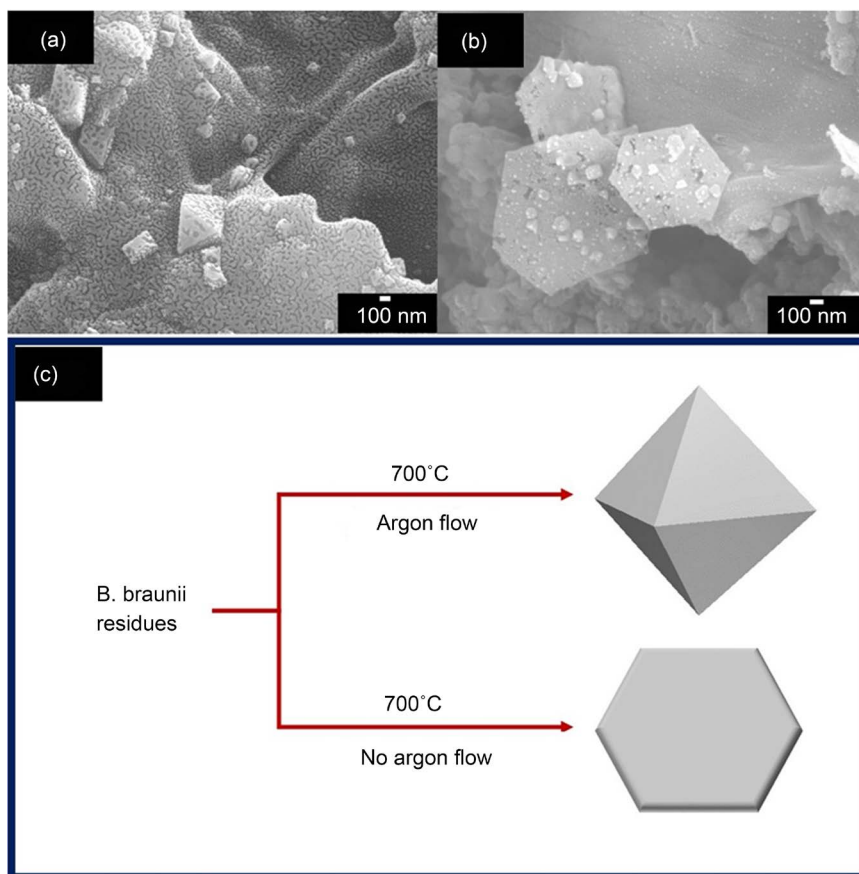


Figure 1. (a) Bulk *B. braunii* residues carbonized at 700°C under argon flow observed under SEM. (b) Bulk *B. braunii* residues carbonized at 700°C with no argon flow observed under SEM. (c) Different carbonization conditions afford to yield different crystal morphology.

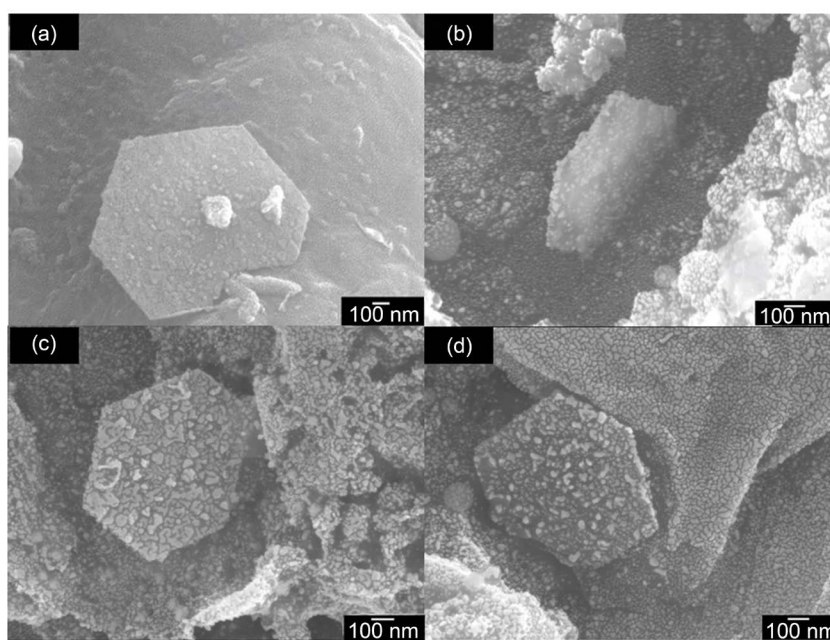


Figure 2. Hexagonal disk structures of carbonized *B. braunii* residues observed under SEM. (a) $\times 40000$; (b) $\times 50000$; (c) $\times 55000$; (d) $\times 55000$.

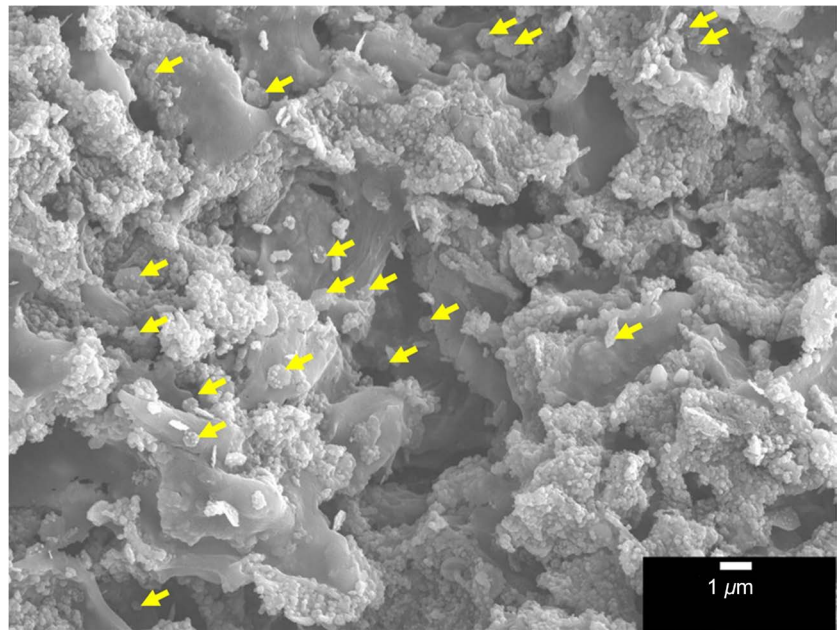


Figure S11. SEM images *B. braunii* residue carbonized at 700°C with no argon flow. Many hexagonal disk pointed by arrows could be observed ($\times 4500$).

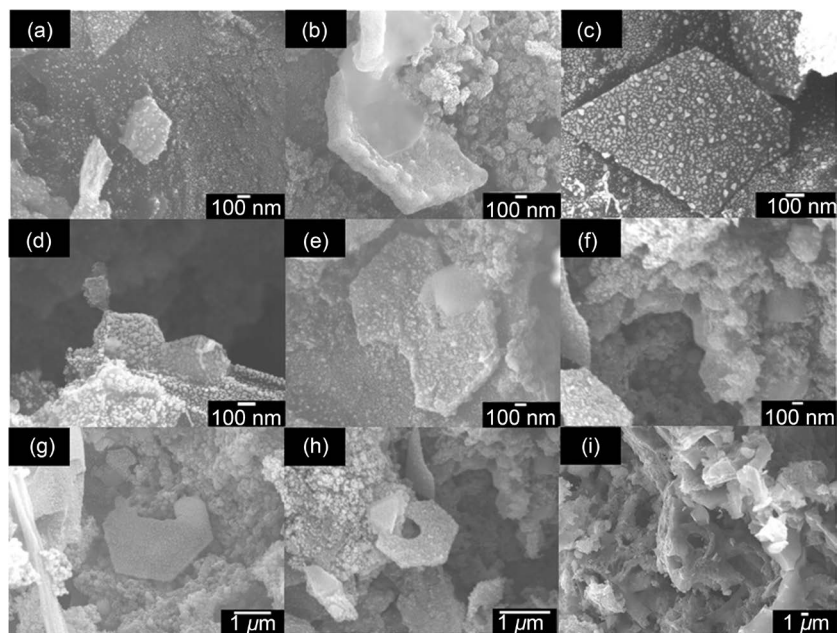


Figure S12. SEM images of hexagonal disks obtained by carbonization of *B. braunii* residue at 700°C with no argon flow (a) $\times 43000$; (b) $\times 40000$; (c) $\times 65000$; (d) $\times 65000$; (e) $\times 45000$; (f) $\times 40000$; (g) $\times 16000$; (h) $\times 22000$; (i) $\times 3000$.

the bulk sample.

3.2. Infrared Absorption Measurement

Figure 3 shows the infrared absorption (IR) spectra of *B. braunii* residue samples carbonized at 700°C with argon and no argon flow, respectively. The absorption peak appears around 1559 cm^{-1} and 1573 cm^{-1} in the sample treated

with argon flow and no argon flow, respectively. This characteristic peak implies the partially formation of graphite inside of the bulk sample. Another prominent peak found around 1041 cm^{-1} and 1573 cm^{-1} in the sample carbonized with argon flow and no argon flow, respectively, ascribes to the vibration of Si-O stretching. These results suggest that carbonization at 700°C with no argon flow can also afford to yield graphite structure and the flocculant polysilicato-iron works as a “glue” in the bulk sample.

3.3. X-Ray Photoelectron Spectroscopy

X-ray photoelectron spectroscopy (XPS) measurement was performed to reveal the components that consists the carbonized samples. As shown in **Figure 4(a)**, both samples mainly consists of carbon and oxygen which peaks appear around 285 eV (C_{1s}), 531 eV (O_{1s}) and 747 eV (O_{KLL}). A slight amount of potassium was detected for the sample treated with argon flow. Significant differences were found in **Figure 4(b)**. Peak at 56 eV , which due to Fe_{3p} , could only be found in the sample treated with argon flow. Other peaks ($\text{Fe}_{2p_{1/2}}$ and $\text{Fe}_{2p_{3/2}}$, 724 eV and 712 eV) of Fe also could only be found in the sample carbonized under argon atmosphere. Peak of magnesium appears at 51 eV in both samples. However, peaks at 153 eV and 102 eV , each representing Si_{2s} and Si_{2p} , respectively, only appeared in the sample carbonized with no argon flow.

3.4. Energy Dispersive X-Ray Spectrometry

The hexagonal disks were analyzed by energy dispersive X-ray spectroscopy to detect the chemical components inside. **Figure 5** shows the results measured for entire region of two samples treated in different conditions. In the previous study, we revealed that carbonization under argon atmosphere would provide an environment for reduction reaction, that, a large amount of Fe would be generated, as shown in **Figure 5(a)**. We can obviously find the difference in **Figure 5(b)** that no significant peak due to Fe could be found in the sample treated with no argon flow. Instead, a large ration of potassium and silicon exist in the sample. These results coincide with the IR and XPS measurement results very well.

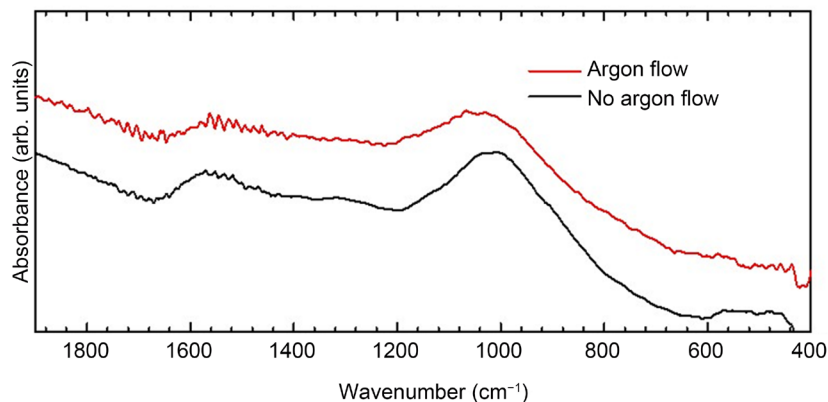


Figure 3. Infrared absorption spectra of *B. braunii* residue carbonized at 700°C in different carbonization conditions.

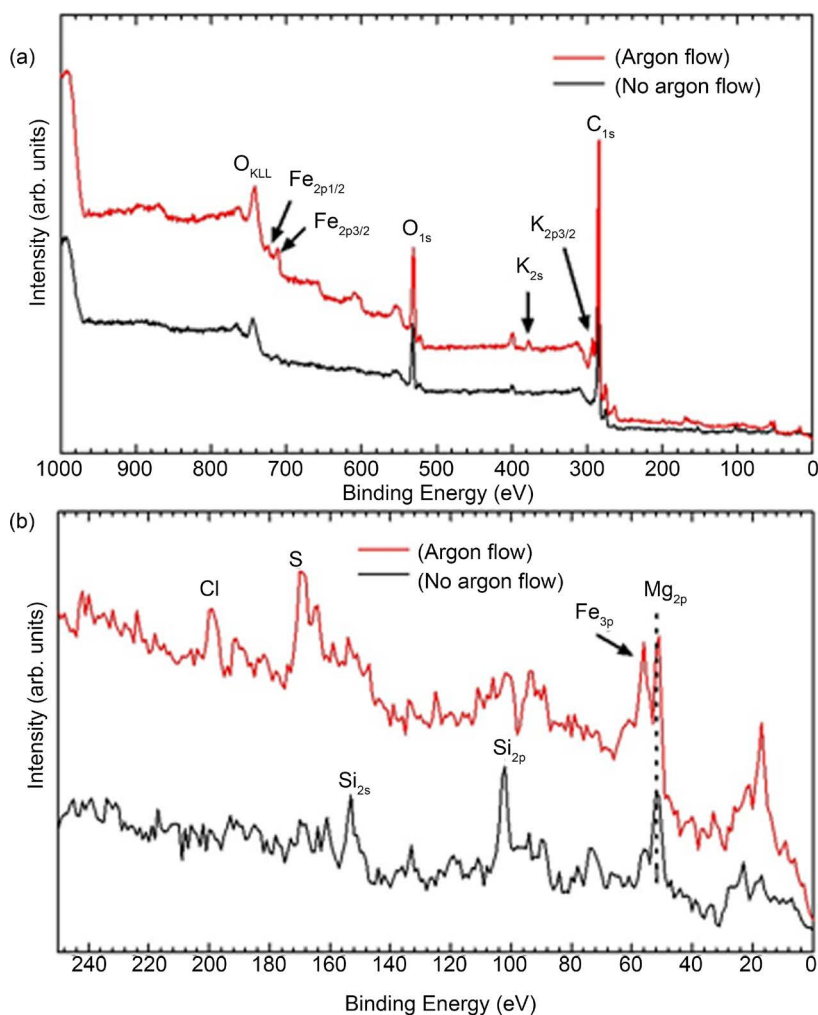


Figure 4. X-ray photoelectron spectra of *B. braunii* residue carbonized at 700°C in different carbonization conditions.

Mapping was carried out for a hexagonal disk. The results in **Figure 6** indicate that components (C, O, Fe, Si, Mg and K) are uniformly dispersed in the sample. Quantitative analysis results of the hexagonal disk are summarized in **Table 1**. The average calculated ration of atoms number of Fe consisted in hexagonal disk is higher than those in entire region. The ration of carbon and oxygen has no significant change in the hexagonal disk and entire region. We found that in each point analysis for the hexagonal disks, no matter with the place, the ratio of number of atoms for Mg, Si and Fe, are nearly fixed as 2:3:6. The hexagonal disk consists of more than 52% of carbon atoms and 25% of oxygen atoms. The carbon atoms basically come from the *B. braunii* cells and oxygen atoms come from *B. braunii* cells, flocculant, and metallic oxide contained in the culture medium.

3.5. Hypothesis of the Formation of Hexagonal Disk

The hexagonal disks are not “regular” hexagon, if we look carefully. Hexagonal disks were randomly selected to investigate the morphology. We recorded the lengths of each side of the hexagonal disk, as summarized in **Table S11**. Six sides

of each hexagonal disk are referred as to “a-f”, respectively, where “a” represents the longest side and others are assigned in the counterclockwise direction. It is worth mentioning that the shortest side of each hexagonal disk can be found only in side “b” and “f”. Moreover, the ratio of the length between the longest and shortest side as calculated, is almost close to 1.5. Three sides “c-e” show almost the same length in each hexagonal disk. The ratio between the longest side and the average length of side “c-e” were calculated and summarized in **Table S11**. Surprisingly, this ratio is almost fixed to 1.2 and is unrelated to the size or thickness of the hexagonal disks. Combining the knowledge we learned from all the results, we would like to build a hypothesis that this anisotropic crystal,

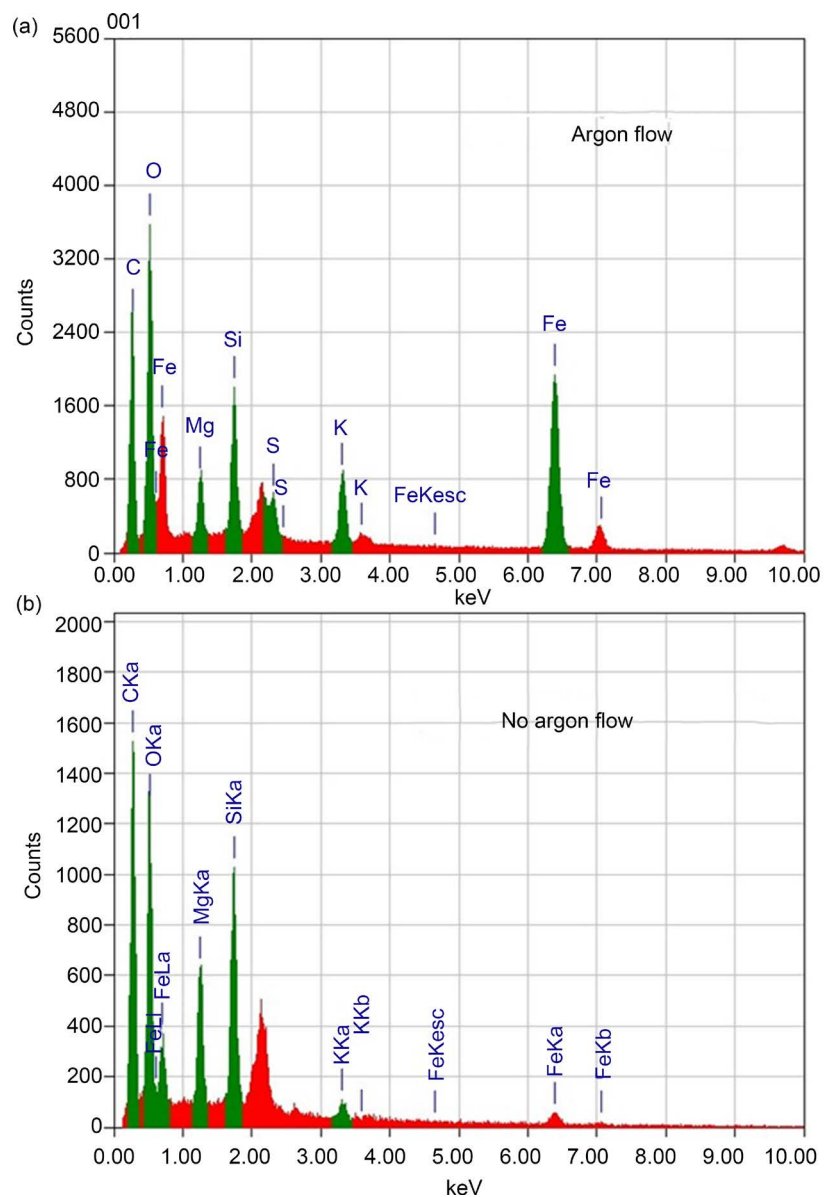


Figure 5. Energy dispersive X-ray spectroscopy of *B. braunii* residue carbonized in different carbonization conditions. (a) For the entire region of sample carbonized at 900°C with argon flow; (b) For the entire region of sample carbonized at 700°C with no argon flow.

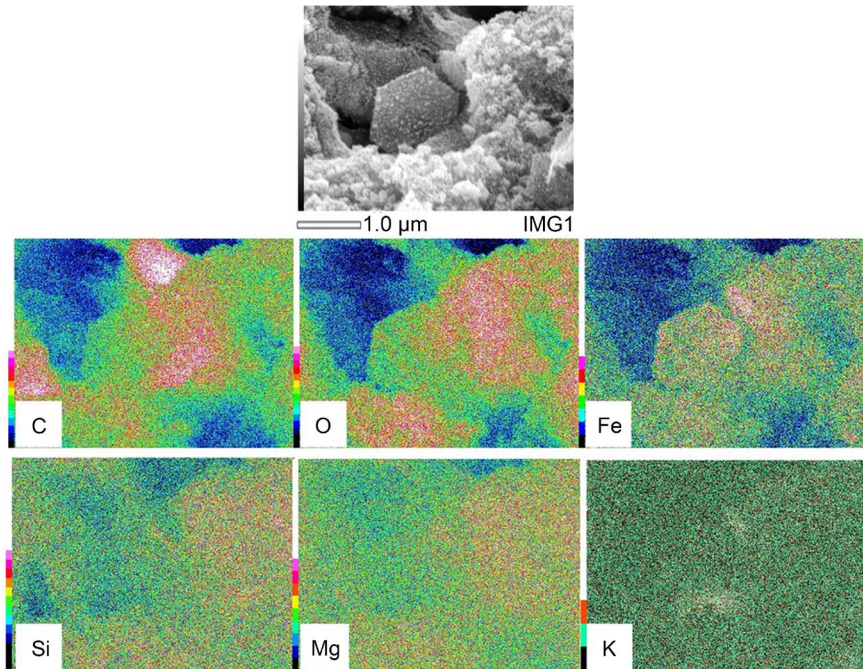


Figure 6. Mapping results of energy dispersive X-ray analysis performed for *B. braunii* residue carbonized at 700°C with no argon flow.

Table 1. Quantitative analysis of *B. braunii* residue carbonized at 700°C with no argon flow.

	Number of atoms (%)	
	Hexagonal disk	Entire region
C	52.41	51.52
O	25.66	27.26
Mg	3.61	5.0
Si	5.43	8.33
K	0.66	0.94
Fe	12.23	7.0
Total	100	100

Table SI1. Summary of the side length of hexagonal disks.

	Hexagonal disk						a/b or a/f	Ave _{c-e}	a/Ave _{c-e}
	a	b	c	d	e	f			
Entry 1	2.4	1.7	1.9	2.1	2.0	1.7	1.41	2.0	1.2
Entry 2	1.9	1.3	1.5	1.5	1.7	1.4	1.46	1.57	1.21

Continued

Entry 3	1.2	0.8	1.1	1.0	0.9	1.1	1.5	1.0	1.2
Entry 4	2.0	1.2	1.9	1.8	1.5	1.7	1.6	1.73	1.16
Entry 5	2.0	1.5	1.7	1.6	1.8	1.3	1.54	1.7	1.17
Entry 6	1.3	0.9	1.1	1.1	1.2	1.0	1.4	1.13	1.15
Entry 7	6.1	4.9	5.0	5.6	5.4	4.7	1.29	5.3	1.15
Entry 8	0.6	0.4	0.55	0.58	0.58	0.37	1.62	0.57	1.05
Entry 9	0.49	0.25	0.45	0.42	0.45	0.40	1.96	0.44	1.11
Entry 10	0.82	0.6	0.7	0.7	0.8	0.5	1.64	0.73	1.12
Entry 11	0.8	0.55	0.7	0.5	0.7	0.52	1.53	0.63	1.27
Entry 12	1.1	0.75	0.68	1.05	0.9	0.6	1.83	1.03	1.07
Entry 13	0.53	0.32	0.48	0.45	0.45	0.49	1.65	0.46	1.08
Entry 14	1.5	1.0	0.98	1.4	1.25	0.9	1.67	1.21	1.24

consisting of large amount of carbon and oxygen, and small amount of Si, Mg, and Fe, is a carbon material with metals and silicon slightly incorporated. Crystal nucleus was formed at the initial stage during the cooling process. EDS line analysis were performed for a hexagonal disk, as shown in **Figure SI3**. Carbon, magnesium, silicon and potassium are uniformly dispersed. However, the oxygen and iron dramatically increase the intensity in the hexagonal shape area. We assume this indicates the existence of iron oxide. Fu *et al.* reported as-synthesized α -Fe₂O₃ microflakes in microscale with hexagonal shape by a hydrothermal method [20].

We assume the micro sized hexagonal disk start from a very small size metal oxide resembling the hexagonal disk. The plausible mechanism is as follows. The 700°C carbonization temperature is high enough to generate a large amount of syngas such as CO, CO₂ and CH₄ during the carbonization process of *B. braunii* residues. Absence of argon flow then creates an environment that mixed gases stagnate in the gold furnace. Subsequent cooling process affords metal oxides deposition; meanwhile syngas act as a carbon source and grow in the order resembling the hexagonal disk shape of metal oxide. The deposited metal oxides may play the role like a substrate for the graphite growth just like the role metal substrates play in chemical vapor deposition method for graphene or any other carbon materials growth [21] [22] [23]. Since more than half of the components in the hexagonal disk are carbon, we refer to this novel 2D hexagonal disk as “Carbon Hexagon”. It is worth mentioning that absence of argon flow prevents the reduction reaction of Fe₂O₃, thus, instead of polygonal structure, hexagonal disk were obtained.

4. Conclusion

Microscale 2D hexagonal disks were found in the *B. braunii* residues carbonized at 700°C with no argon flow. These hexagonal disks have self-similarity which is not related to size or thickness. In this study, we emphasized the importance of

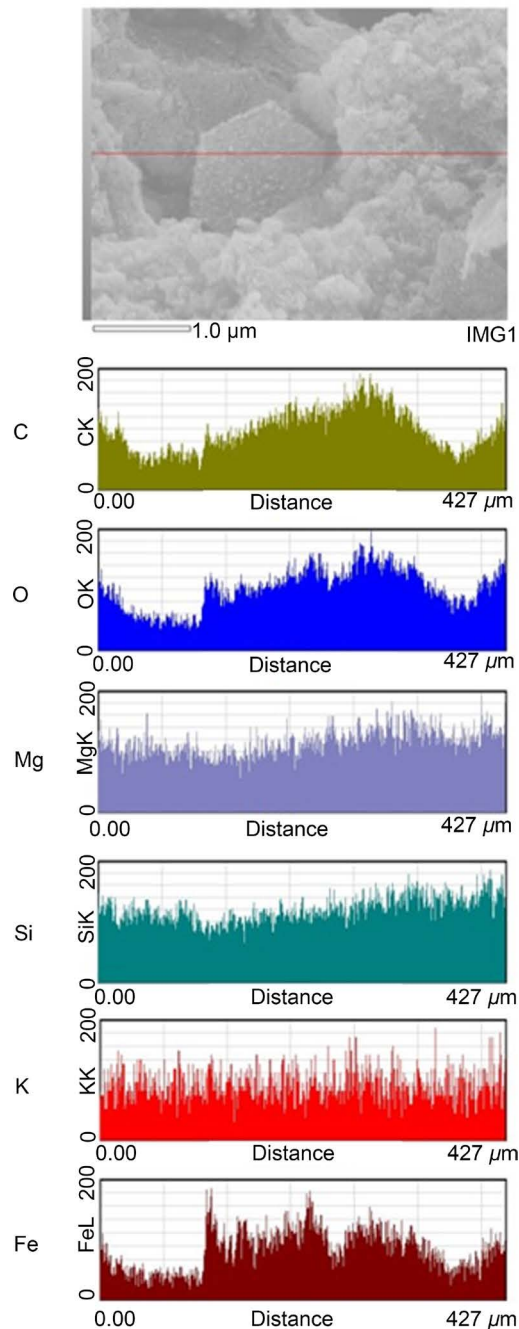


Figure SI3. EDS line analysis of a hexagonal disk obtained by carbonization of *B. braunii* residue at 700°C with no argon flow.

argon flow that would affect the properties of final carbon material. 2D hexagonal shape has high anisotropy and large surface area, thus is promised to be the building blocks for functional materials. Recently, self-assembled structures of graphene or graphite are studied in the carbon material science because the dimensional anisotropy can significantly affect the thermal, optical, and electronic properties of the material [24]. The hexagonal disk can be a good candidate for the micro-size electronic devices. This report is the first discovery of the

hexagonal disks in the biomass residues treated by carbonization. This study not only opens a new avenue for the discharged biomass material from the point of view of materials science, but also consummates the new energy system based on microalgae.

Acknowledgements

We appreciate the nice glasswork from Engineering Workshop, Research Facility Center for Science and Technology, Open Facility Network Office, University of Tsukuba. We are especially grateful to Dr. Shinichi Ito for his great support of assembling the furnace. A part of this work was supported by NIMS microstructural characterization platform as a program of “Nanotechnology Platform” of the Ministry of Education, Culture, Sports, Science and Technology (MEXT), Japan. We also thank Tsukuba Research Center for Interdisciplinary Materials Science (TIMS), University of Tsukuba, Japan.

References

- [1] Halim, R., Gladman, B., Danquah, M.K. and Webley, P.A. (2010) Oil Extraction from Microalgae for Biodiesel Production. *Bioresource Technology*, **102**, 178-185. <https://doi.org/10.1016/j.biortech.2010.06.136>
- [2] Pragma, N., Pandey, K.K. and Sahoo, P.K. (2013) A Review on Harvesting, Oil Extraction and Biofuels Production Technologies from Microalgae. *Renewable and Sustainable Energy Reviews*, **24**, 159-171. <https://doi.org/10.1016/j.rser.2013.03.034>
- [3] Huang, J., Xia, J., Jiang, W., Li, Y. and Li, J. (2015) Biodiesel Production from Microalgae Oil Catalyzed by a Recombinant Lipase. *Bioresource Technology*, **180**, 47-53. <https://doi.org/10.1016/j.biortech.2014.12.072>
- [4] Song, C., Chen, G., Ji, N., Liu, Q., Kansha, Y. and Tsutsumi, A. (2015) Biodiesel Production Process from Microalgae Oil by Waste Heat Recovery and Process Integration. *Bioresource Technology*, **193**, 192-199. <https://doi.org/10.1016/j.biortech.2015.06.116>
- [5] Voloshin, R.A., Rodionova, M.V., Zharmukhamedov, S.K., Veziroglu, T.N. and Al-lakhverdiev, S.I. (2016) Review: Biofuel Production from Plant and Algal Biomass. *International Journal of Hydrogen Energy*, **41**, 17257-17273. <https://doi.org/10.1016/j.ijhydene.2016.07.084>
- [6] Singh, J. and Gu, S. (2010) Commercialization Potential of Microalgae for Biofuels Production. *Renewable and Sustainable Energy Reviews*, **14**, 2596-2610. <https://doi.org/10.1016/j.rser.2010.06.014>
- [7] Singh, B., Guldhe, A., Rawat, I. and Bux, F. (2014) Towards a Sustainable Approach for Development of Biodiesel from Plant and Microalgae. *Renewable and Sustainable Energy Reviews*, **29**, 216-245. <https://doi.org/10.1016/j.rser.2013.08.067>
- [8] Rizzo, A.M., Prussi, M., Bettucci, L., Libelli, I.M. and Chiaramonti, D. (2013) Characterization of Microalga *Chlorella* as a Fuel and Its Thermogravimetric Behavior. *Applied Energy*, **102**, 24-31. <https://doi.org/10.1016/j.apenergy.2012.08.039>
- [9] Maity, J.P., Bundschuh, J., Chen, C. and Bhattacharya, P. (2014) Microalgae for Third Generation Biofuel Production, Mitigation of Greenhouse Gas Emissions and Wastewater Treatment: Present and Future Perspectives—A Mini Review. *Energy*, **78**, 104-113. <https://doi.org/10.1016/j.energy.2014.04.003>
- [10] Menger-Krug, E., Niederste-Hollenberg, J. and Hillenbrand, T. (2012) Integration

- of Microalgae Systems at Municipal Wastewater Treatment Plants: Implications for Energy and Emission Balances. *Environmental Science and Technology*, **46**, 11505-11514. <https://doi.org/10.1021/es301967y>
- [11] Shimamura, R., Watanabe, S., Sagakura, Y., Shiho, M., Kaya, K. and Watanabe, M.M. (2012) Development of *Botryococcus* Seed Culture System for Future Mass Culture. *Procedia Environmental Sciences*, **15**, 80-89. <https://doi.org/10.1016/j.proenv.2012.05.013>
- [12] Fu, X., Li, D., Chen, J., Zhang, Y., Huang, W., Zhu, Y., et al. (2013) A Microalgae Residue Based Carbon Solid Acid Catalyst for Biodiesel Production. *Bioresource Technology*, **146**, 767-770. <https://doi.org/10.1016/j.biortech.2013.07.117>
- [13] Zhao, B., Ma, J., Zhao, Q., Laurens, L., Jarvis, E., Chen, S., et al. (2014) Efficient Anaerobic Digestion of Whole Microalgae and Lipid-Extracted Microalgae Residues for Methane Energy Production. *Bioresource Technology*, **161**, 423-430. <https://doi.org/10.1016/j.biortech.2014.03.079>
- [14] Bui, H., Tran, K. and Chen, W. (2016) Pyrolysis of Microalgae Residues—A Kinetic Study. *Bioresource Technology*, **199**, 362-366. <https://doi.org/10.1016/j.biortech.2015.08.069>
- [15] Chen, W., Huang, M., Chang, J. and Chen, C. (2014) Thermal Decomposition Dynamics and Severity of Microalgae Residues in Torrefaction. *Bioresource Technology*, **169**, 258-264. <https://doi.org/10.1016/j.biortech.2014.06.086>
- [16] Wang, A., Demura, M., Watanabe, M.M., Ohara, K., Kashiwagi, T., Kadowaki, K., et al. (2017) Surface Observations and Magnetism of Oil-Extracted *Botryococcus braunii* Residues before and after Carbonization. Submitted.
- [17] Yonezawa, N., Matsuura, H., Shiho, M., Kaya, K. and Watanabe, M.M. (2012) Effects of Soybean Curd Wastewater on the Growth and Hydrocarbon Production of *Botryococcus braunii* Strain BOT-22. *Bioresource Technology*, **109**, 304-307. <https://doi.org/10.1016/j.biortech.2011.07.090>
- [18] Ishimatsu, A., Matsuura, H., Sano, T., Kaya, K. and Watanabe, M.M. (2012) Biosynthesis of Isoprene Units in the C₃₄ Botryococcene Molecule Produced by *Botryococcus braunii* Strain Bot-22. *Procedia Environmental Sciences*, **15**, 56-65. <https://doi.org/10.1016/j.proenv.2012.05.010>
- [19] Polysilicate-Iron Mainly Contains [SiO₂]_n-Fe₂O₃, According to the MSDS Sheet Provided by Nankai Chemical. Other Additives Are FeCl₃aq, Na₂SiO₃, H₂SO₄.
- [20] Fu, L., Jiang, J., Xu, C. and Zhen, L. (2012) Synthesis of Hexagonal Fe Microflakes with Excellent Microwave Absorption Performance. *CrystEngComm*, **14**, 6827-6832. <https://doi.org/10.1039/c2ce25836f>
- [21] Lee, C.J., Park, J. and Yu, J.A. (2002) Catalyst Effect on Carbon Nanotubes Synthesized by Thermal Chemical Vapor Deposition. *Chemical Physics Letters*, **360**, 250-255. [https://doi.org/10.1016/S0009-2614\(02\)00831-X](https://doi.org/10.1016/S0009-2614(02)00831-X)
- [22] Shyu, Y. and Hong, F.C.N. (2001) The Effects of Pre-Treatment and Catalyst Composition on Growth of Carbon Nanofibers at Low Temperature. *Diamond and Related Materials*, **10**, 1241-1245. [https://doi.org/10.1016/S0925-9635\(00\)00550-1](https://doi.org/10.1016/S0925-9635(00)00550-1)
- [23] Chee, S.W. and Sharma, R. (2012) Controlling the Sized and the Activity of Fe Particles for Synthesis of Carbon Nanotubes. *Micron*, **43**, 1181-1187. <https://doi.org/10.1016/j.micron.2012.01.008>
- [24] Lee, M.V., Hiura, H., Kuramochi, H. and Tsukagoshi, K. (2012) Concerted Chemical-Mechanical Reaction in Catalyzed Growth of Confined Graphene Layers into Hexagonal Disks. *The Journal of Physical Chemistry C*, **116**, 9106-9113. <https://doi.org/10.1021/jp301580t>

Submit or recommend next manuscript to SCIRP and we will provide best service for you:

Accepting pre-submission inquiries through Email, Facebook, LinkedIn, Twitter, etc.

A wide selection of journals (inclusive of 9 subjects, more than 200 journals)

Providing 24-hour high-quality service

User-friendly online submission system

Fair and swift peer-review system

Efficient typesetting and proofreading procedure

Display of the result of downloads and visits, as well as the number of cited articles

Maximum dissemination of your research work

Submit your manuscript at: <http://papersubmission.scirp.org/>

Or contact msce@scirp.org